The cell adhesion molecule BT-IgSF is essential for a functional blood–testis barrier and male fertility in mice

Received for publication, September 26, 2017, and in revised form, November 7, 2017 Published, Papers in Press, November 9, 2017, DOI 10.1074/jbc.RA117.000113

Laura Pelz[‡], Bettina Purfürst[§], and Fritz G. Rathjen[‡1]

From the [‡]Department of Neurobiology and the [§]Core Facility for Electron Microscopy, Max Delbrück Center for Molecular Medicine, Helmholtz Association, D-13092 Berlin, Germany

Edited by Xiao-Fan Wang

The Ig-like cell adhesion molecule (IgCAM) BT-IgSF (brain- and testis-specific Ig superfamily protein) plays a major role in male fertility in mice. However, the molecular mechanism by which BT-IgSF supports fertility is unclear. Here, we found that it is localized in Sertoli cells at the blood–testis barrier (BTB) and at the apical ectoplasmic specialization. The absence of BT-IgSF in Sertoli cells in both global and conditional mouse mutants (*i.e.* AMHCre and Rosa26CreERT2 lines) resulted in male infertility, atrophic testes with vacuolation, azoospermia, and spermatogenesis arrest. Although transcripts of junctional proteins such as connexin43, ZO-1, occludin, and claudin11 were up-regulated in the absence of BT-IgSF, the functional integrity of the BTB was impaired, as revealed by injection of a BTB-impermeable component into the testes under *in vivo* conditions. Disruption of the BTB coincided with mislocalization of connexin43, which was present throughout the seminiferous epithelium and not restricted to the BTB as in wild-type tissues, suggesting impaired cell–cell communication in the BT-IgSF–KO mice. Because EM images revealed a normal BTB structure between Sertoli cells in the BT-IgSF–KO mice, we conclude that infertility in these mice is most likely caused by a functionally impaired BTB. In summary, our results indicate that BT-IgSF is expressed at the BTB and is required for male fertility by supporting the functional integrity of the BTB.

BT-IgSF (brain- and testis-specific Ig superfamily protein, also termed IgSF11) is a transmembrane Ig-like cell adhesion molecule (IgCAM)[2] with a widespread tissue distribution that is preferentially expressed in brain and testis (1, 2). BT-IgSF shares with coxsackievirus and adenovirus receptor (CAR), endothelial cell-selective adhesion molecule, and CLMP (CAR-like membrane protein) an identical overall domain organization with a membrane-distal V-type domain and a membrane-proximal C2-type domain (3). Adhesion assays with heterologous cells demonstrated that BT-IgSF promotes homotypic binding between neighboring cells similar to its related proteins CAR or CLMP (4, 5). BT-IgSF also contains a PDZ-binding motif at its C terminus to facilitate interactions with intracellular proteins including binding to PSD95 (6). In the mouse brain, BT-IgSF is highly expressed in the mature dentate gyrus of the hippocampus, and knockdown experiments revealed that BT-IgSF is implicated in α-amino-3-hydroxy-5-methyl-4-isoxazolepropionic acid receptor (AMPAR)-mediated synaptic transmission and plasticity (6). For non-neuronal cells, a critical role for BT-IgSF in promoting the migration of melanophores and their precursors has been described in zebrafish and *Neolamprologus meeli* (4, 7).

Despite strong expression of BT-IgSF transcripts in the testes, its function here is currently not well understood. In seminiferi tubuli of the testes, cell–cell interactions and extensive restructuring of cell–cell contacts mediated by number of proteins including IgCAMs are indispensable for the sperm maturation and maintenance of tissue homeostasis. With the help of mouse genetics, we uncovered a role of BT-IgSF in the retention of the blood–testis barrier, which is formed by cell–cell junctions of the Sertoli cells including tight, adherens, and gapjunctions and desmosomes (for review see Refs. 8 and 9). Sertoli cells stretch from the basal site of the seminiferous epithelium to the lumen and divide the epithelium into two compartments. The BTB restricts blood contact to the basal side of the seminiferous epithelium and thereby protects meiotic germ cells and spermatids from autoimmune reactions and toxins. Alterations in the expression of proteins of the BTB, such as Claudin11, Occludin, ZO-2, and Cx43 can lead to severe defects in spermatogenesis, because deletion of these proteins causes infertility in mice (10–15).

The cascade of sperm generation also requires the Sertoli cells as nursing cells by creating an intimate contact between Sertoli and germ cells, by providing a suitable environment for germ cell differentiation, and by establishing a hormonal balance (16). Spermatogonial stem cells and premeiotic spermatogonia that are located in the basal part of the testes differentiate into preleptotene and leptotene spermatocytes, which transverse through the BTB to the adluminal part where meiosis and the spermiogenesis occurs. The process of cell movement requires a dynamic disassembly and assembly of cell–cell junctions between Sertoli cells and between Sertoli and germ cells. There is another important cell–cell contact site between Sertoli and germ cells called the apical ectoplasmic specialization

This work was supported by Max Delbrück Center grants. The authors declare that they have no conflicts of interest with the contents of this article. The content is solely the responsibility of the authors and does not necessarily represent the official views of the National Institutes of Health.

This article contains Figs. S1 and S2.

[1] To whom correspondence should be addressed. E-mail: rathjen@mdc-berlin.de.

[2] The abbreviations used are: IgCAM, Ig-like cell adhesion molecule; AMH, anti-Müllerian hormone; BTB, blood–testis barrier; CAR, coxsackievirus and adenovirus receptor; Cx43, Connexin 43; ES, ectoplasmic specialization; WT1, Wilms tumor 1; ZO-1, zona occludens-1; KOMP, Knock-Out Mouse Project; H&E, hematoxylin and eosin; qRT-PCR, quantitative RT-PCR; LH, luteinizing hormone; PFA, paraformaldehyde.

(ES). The ES is a testis-specific actin-based anchoring junction complex, composed of adherens junctions, focal adhesion complex, and tight junction proteins (17). The structure of the ES surrounds the head of spermatids and is the only anchor for developing elongating and elongated spermatids (18).

In this study, we investigated the role of the IgCAM BT-IgSF in the murine testes. We showed that the IgCAM BT-IgSF is a novel component of the BTB that is essential for its functional integrity. The loss of BT-IgSF leads to infertility because of azoospermia caused by an impaired function of the BTB despite the fact that ZO-1, Occludin, and Cx43 transcripts were found to be up-regulated. Most importantly, Cx43 is mislocalized in the seminiferi tubuli of BT-IgSF knockouts, suggesting a disturbed cell–cell communication.

Results

BT-IgSF is expressed at the blood–testis barrier and apical ectoplasmic specialization: Loss of BT-IgSF leads to atrophic testes and male infertility

To study the localization of BT-IgSF in the testes, a polyclonal antibody to the extracellular region of mBT-IgSF was generated in rabbits. BT-IgSF was localized on the basal site of the seminiferi tubuli and associated with Sertoli cells close to its nucleus (Fig. 1, *A* and *B*, *arrowheads*). At the BTB, it co-localizes partly with connexin43 (Fig. 1*E*) and more extensively with ZO-1 (Fig. 1*F*). Furthermore, at the adluminal compartment at or around the acrosome of elongated spermatids (Fig. 1, *A* and *B*, *arrows*), co-localization with Espin was observed, indicating expression at the apical ectoplasmic specialization: an actin-based cell–cell anchoring junction (Fig. 1*D*). The localization on the sperm is further supported by the presence of BT-IgSF staining in the ductules of the epididymis (Fig. 1*C*). Even at higher magnifications (Fig. S2*D*), it remains unclear whether BT-IgSF protein is also expressed on germ cells because the thin cytoplasmic arms of Sertoli cells extend toward the lumen.

To elucidate the role of BT-IgSF in the testis, we initially analyzed a non-conditional BT-IgSF knock-out mouse (Fig. S1). We observed that the testis size of BT-IgSF knock-out mice was significantly reduced compared with wild-type and heterozygous animals (Fig. 1, *G* and *H*), whereas other organs and the overall organization seem not to be affected. Breeding of BT-IgSF knock-out males to C57BL/6N wild-type females (five males with two females each) did not result in any offspring, although vaginal plugs were observed, indicating normal mating behavior but infertility. Heterozygous males and BT-IgSF knock-out females (nine females inspected) were fertile, suggesting that infertility is restricted to homozygous males.

In H&E-stained sections, atrophic testes with vacuolar degeneration of the semininferi tubuli (Fig. 1*I*, *asterisk*) and Sertoli cell cytoplasmic extensions (Fig. 1*I*, *arrowhead*) were observed in BT-IgSF–deficient mice. Diameter of BT-IgSF knock-out tubuli were significantly smaller (158.22 ± 3.41 μm) compared with wild-type tubuli (212.39 ± 2.83 μm) (Fig. S2*A*). No sperms were detected in the lumen of homozygous knock-out animals (Fig. 1*I*, enlarged image for details, *blue arrow*). In contrast, multinucleated cells at the luminal site were found (Fig. 1*I*, *arrow*).

Analysis of testis preparations, stained for DNA with DAPI, by flow cytometry showed that BT-IgSF–deficient testes lacked haploid cells with 1C DNA content (Fig. 1*J*). This observation further demonstrated that loss of BT-IgSF leads to azoospermia.

The loss of BT-IgSF leads to spermatogenic arrest after meiosis I

The lack of haploid cells in the seminiferi tubuli indicates an arrest in spermatogenesis and a disturbance of meiosis. To determine the exact stage of arrest, expression of genes transcribed during spermatogenesis were measured by qRT-PCR (19–21).

The expression of Piwil2 did not significantly differ between wild-type and BT-IgSF knock-out mice (Fig. 2*A*), suggesting that the number of stem cells are not changed in abundance. A slight tendency toward an increased stem cell amount in the knock-out was detected. However, the transcripts for germ cells in the mid-pachytene stage and late pachytene stages, HoxA4 and Cdc25c, respectively, were significantly reduced. In contrast, marker for the overall pachytene stage (Sycp3) and for meiotic cells in general (Dazl) were up-regulated, suggesting an increased cell number between the stem cell stage and the mid-pachytene stage. Transcripts for postmeiotic markers (Akap4 and Prm1), which are only expressed in haploid spermatids, were not detected at all in knock-out testes. These expression data also indicated a complete lack of spermatids and sperms.

Next, we investigated whether the changes in gene expression have an impact on meiosis I. Arrest in meiosis I is often caused by failed pairing of homologous chromosomes. To examine whether this pairing works out properly in BT-IgSF KO males, stainings with antibodies against SYCP3 or γH2AX were performed on testis sections. SYCP3 is a marker for the axial element of the synaptonemal complex from zygotene to pachytene stage during meiosis I, and phosphorylated H2AX (γH2AX) is expressed from leptotene on and later marks the silenced sex body (meiotic sex chromosome inactivation) (22, 23). Wild-type and knock-out testis show SYCP3 expression, although in slightly different patterns, which can be attributed to the disturbed testis morphology in BT-IgSF–deficient mice. In both genotypes γH2AX was co-expressed with SYCP3 at early pachytene, indicated by diffuse distribution (Fig. 2*B*, *arrows*), as well as late pachytene, implied by a restricted expression at the inactivated X-chromosome (Fig. 2*B*, *arrowheads*). In the knock-out testes, all meiotic cells expressed γH2AX, indicating that all of these cells are in meiosis I. In meiosis II, which represents a mitosis, γH2AX is normally not expressed (Fig. S2*E*). Therefore, these results show that in BT-IgSF–deficient germ cells, meiosis I appears to be properly carried out and that the spermatogenic arrest most likely occurs after meiosis I.

Absence of BT-IgSF caused irregular arms of Sertoli cells but did not affect the hormonal balance

To assess implications of BT-IgSF absence on Sertoli cells, we analyzed the localization of intermediate filament vimentin in testis sections, which showed irregular and disturbed cytoplasmic arms of Sertoli cells in BT-IgSF knock-out mice (Fig. 3*A*). However, the localization and the number of Sertoli cells, as detected by nuclear staining with Wilms tumor 1 (WT1), appears not to be affected (Fig. 3*B*).

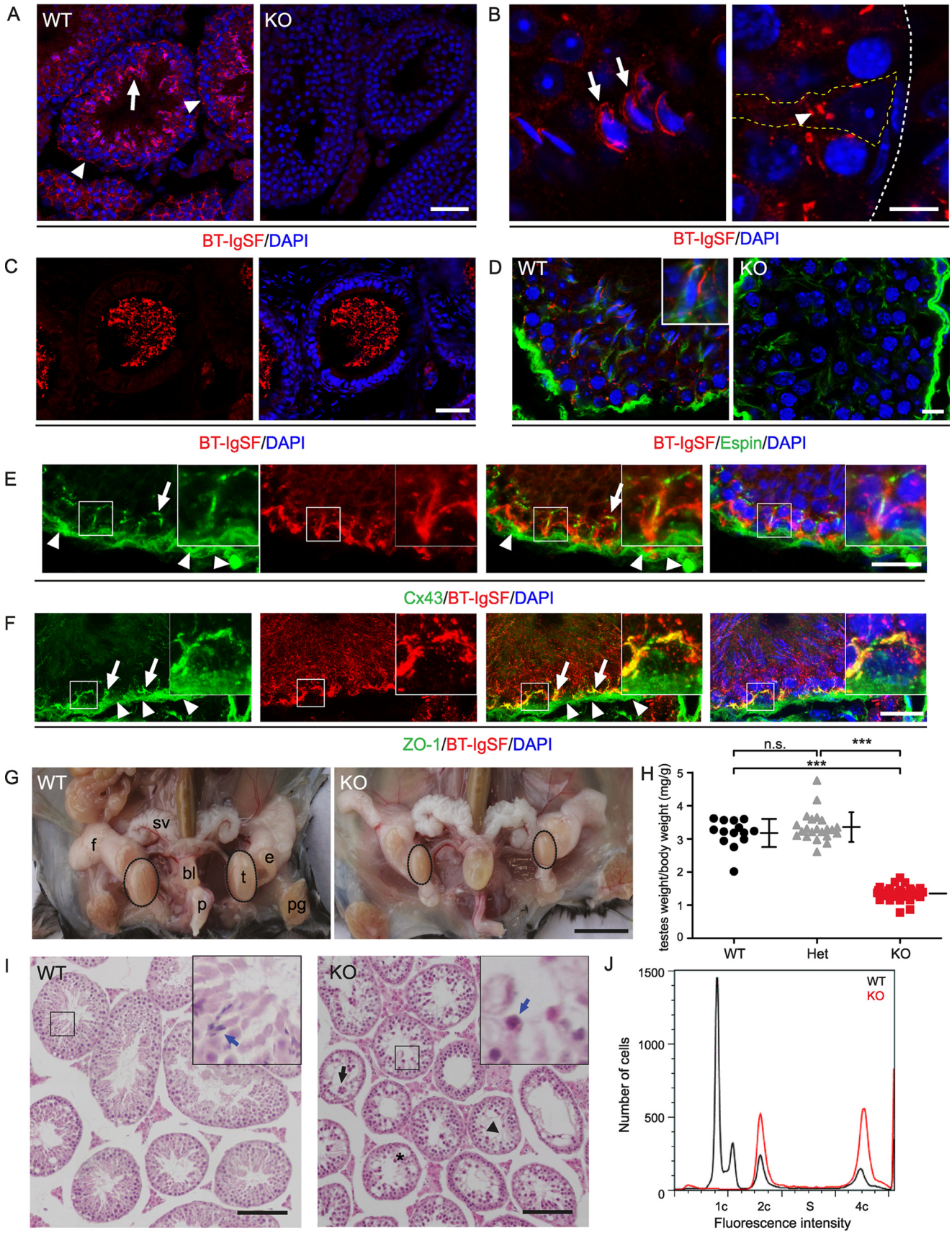
A
WT
KO
BT-IgSF/DAPI
B
BT-IgSF/DAPI
C
BT-IgSF/DAPI
D
WT
KO
BT-IgSF/Espin/DAPI
E
Cx43/BT-IgSF/DAPI
F
ZO-1/BT-IgSF/DAPI
G
WT
KO
sv
f
bl
t
e
p
pg
H
n.s.
***
***
testes weight/body weight (mg/g)
0
1
2
3
4
5
WT
Het
KO
I
WT
KO
J
WT
KO
Number of cells
0
500
1000
1500
1c
2c
S
4c
Fluorescence intensity

Analysis of cell death by an antibody against active caspase-3 revealed a slight increase of positive cells in BT-IgSF knock-out, which, however, did not reach statistical significance. On the basis of their localization inside the tubuli and the presence of cytoplasmic arms, apoptotic cells in knock-out testes were considered as Sertoli cells (Fig. 3, *C* and *D*).

Azoospermia caused by Sertoli cells might affect the hormonal hypothalamic–pituitary axis in BT-IgSF– deficient males. Therefore, the level of the luteinizing hormone (LH), the follicle-stimulating hormone (FSH), and testosterone in the blood of wild-type and BT-IgSF knock-out mice were measured by an ELISA– based technique. No significant differences in LH, FSH, and testosterone between genotypes were detected (Fig. 3*E*). Differences in the LH levels between knock-out individuals are probably due to episodically discontinuous pulses of LH, which have been previously described (24). These findings indicate that a disturbed hormonal balance does not contribute to male infertility in BT-IgSF– deficient mice.

Loss of BT-IgSF resulted in severe disruption of the BTB and changed the expression of BTB proteins

The expression and its subcellular localization of BT-IgSF in Sertoli cells prompted us to analyze BTB integrity in BT-IgSF knock-out mice by injecting EZ-Link Sulfo-NHS-LC-Biotin, which is BTB–impermeable, into the testis in an *in vivo* situation (25). The injected EZ-Link Sulfo-NHS-LC-Biotin was visualized after fixation with streptavidin-coupled Cy5 in cryostat sections. In wild-type testis, biotin staining outlined the basal spermatogonia but was not detectable in other cell layers (Fig. 4*A*). In contrast, in BT-IgSF KO testis, the biotin signal was less sharp in the basal compartment and was additionally detected in other cell layers, indicating a disruption of the BTB.

The BTB consists of several cell– cell contact proteins forming tight junctions, gap junctions, and adherens junctions (for review see Refs. 9 and 26). Therefore, we analyzed the expression of mRNAs of proteins involved in the BTB by qRT-PCR and observed striking differences between wild-type and BT-IgSF knock-out testes. The tight junction transcripts Cldn11, Occludin, and ZO-1 were significantly up-regulated in knock-out testes (Fig. 4*B*). In immunofluorescence stainings of testis sections, ZO-1 protein appears slightly enhanced, and its localization appears less organized at the BTB in comparison with wild-type (Fig. 4*E*). Similarly to the tight junction proteins, the mRNA of Cx43, the most abundantly expressed gap junctional protein in testes, is also up-regulated in BT-IgSF knock-out testes (Fig. 4*B*). This increase was also clearly detected in immunofluorescence stainings. Moreover and most interestingly, Cx43 was found to localize throughout the knock-out tubule and not to be restricted to the BTB, whereas in the wild-type Cx43 is sharply located at the basal site of the seminiferi tubuli at the BTB (Fig. 4*F*). Furthermore, the phosphorylation status of Cx43 was increased in BT-IgSF– deficient testes (Fig. 4, *C* and *D*), although with some variabilities.

In electron microscopy of testis sections, vacuolation (Fig. 4*G*, *red outlines*), as well as the lack of sperm and a disorganization of the epithelium, was detected in BT-IgSF knockouts. However, no differences in the ultrastructure of the BTB of wild-type and knock-out testis was detected at this level (Fig. 4*G*, *arrowheads*); all sections showed intact BTB structures including "new" and "old" BTBs behind and ahead of the pachytene spermatocytes, respectively, suggesting that BTB formation can occur in the absence of BT-IgSF but that its functionality is disturbed (Fig. S2*G*).

Sertoli cell–specific expression of BT-IgSF is essential for male fertility

To further substantiate that BT-IgSF expression in Sertoli cells is needed for proper testis morphology and fertility, we inactivated BT-IgSF by crossing a floxed BT-IgSF allele to AMH^{Cre} to specifically knock-out the BT-IgSF gene in Sertoli cells only. In BT-$IgSF^{flx/flx}$, AMH^{Cre} males the exact same phenotype as in the global knock-out was observed. The animals showed reduced testis weight (Fig. 5*A*), together with atrophic morphology in seminiferous tubules (Fig. 5*B*) and azoospermia (Fig. 5*D*). Knock-out of BT-IgSF in Sertoli cells was proven by immunofluorescence stainings with antibodies to BT-IgSF (Fig. 5*C*, *arrowheads*). Interestingly, the stainings showed minimal residual BT-IgSF expression, but not in Sertoli cells. The results of the AMH-conditional knock-out support that the expression of BT-IgSF in Sertoli cells is essential for male fertility.

Loss of BT-IgSF in adulthood also affects spermatogenesis

To exclude overall developmental defects on the absence of BT-IgSF, we developed a conditional knock-out in which BT-IgSF can be depleted at any chosen stage by the administration of tamoxifen (BT-$IgSF^{flx/flx}$; Rosa26CreERT2). Inactivation of BT-IgSF in sexually mature males (8–12 weeks old) by tamoxifen treatment at 5 consecutive days resulted in a testis weight

Figure 1. BT-IgSF knock-out males reveal a disturbed testis morphology and are infertile. *A*, immunofluorescence staining of wild-type and BT-IgSF knock-out testis sections with a BT-IgSF antibody. *Arrow*, expression at the adluminal side, in elongated spermatids; *arrowheads*, expression at the basal side, in Sertoli cells; *scale bar*, 50 μm. *B*, immunofluorescence staining of wild-type testis sections against BT-IgSF. *Arrows*, expression at elongated spermatids at the apical ES; *arrowhead*, expression at the basal side (marked by *white dashed line*), in Sertoli cells (indicated by *yellow dashed line*); *scale bar*, 5 μm. *C*, immunofluorescence staining of epididymis sections show labeling of mature sperm. *Scale bar*, 50 μm. *D*, immunofluorescence staining of testis sections show BT-IgSF co-localized with Espin at the apical ES. *Scale bar*, 10 μm. *E*, immunofluorescence staining of wild-type testis sections against BT-IgSF and mouse anti-Cx43; Cx43 co-localizes partly with BT-IgSF. *Arrow*, specific expression at the basal side (please compare with staining of rabbit anti-Cx43 Fig. 4*F*); *arrowheads*, unspecific staining of a band around the tubuli by the secondary goat anti-mouse A488 antibody (see also S2F); *scale bar*, 25 μm. *F*, immunofluorescence staining of wild-type testis sections against BT-IgSF and mouse anti-ZO-1. Note the strong co-localization of BT-IgSF and ZO-1. *Arrows*, specific expression at the basal side (please compare with staining of rabbit anti-ZO-1 Fig. 4*E*); *arrowheads*, unspecific staining of a band around the tubuli by the secondary goat anti-mouse A488 antibody (see also S2F); *scale bar*, 20 μm. *G*, BT-IgSF knock-out animals exhibit smaller testes. *bl*, bladder; *e*, epididymis; *f*, fat; *p*, penis; *pg*, preputial gland; *sv*, seminal vesicle; *t*, testis; *scale bar*, 5 mm. *H*, knock-out testes showed a significantly decreased wet weight compared with wild-type and heterozygous testes; p value < 0.001 (one-way analysis of variance with Bonferroni correction; WT animals, $n = 14$; heterozygous animals, $n = 22$; KO animals, $n = 30$). The data are shown as means $\pm$ S.D. *I*, H&E staining of methacrylate-sections show atrophic testes of BT-IgSF knock-out animals. *Black arrow*, multinucleated cells; *arrowheads*, Sertoli cell cytoplasmic extensions; *asterisk*, vacuolar degeneration; *scale bar*, 100 μm. *Insets* shows the lack of sperms in KO animals at higher magnification (*blue arrow*). *J*, flow cytometric analysis of testis cells, stained with DAPI, shows the lack of haploid chromatin containing cells in BT-IgSF knockouts (*red*). *1c*, haploid, 23 chromatids; *2c*, haploid, 23 chromosomes; *S*, S phase; *4c*, diploid, 46 chromosomes.

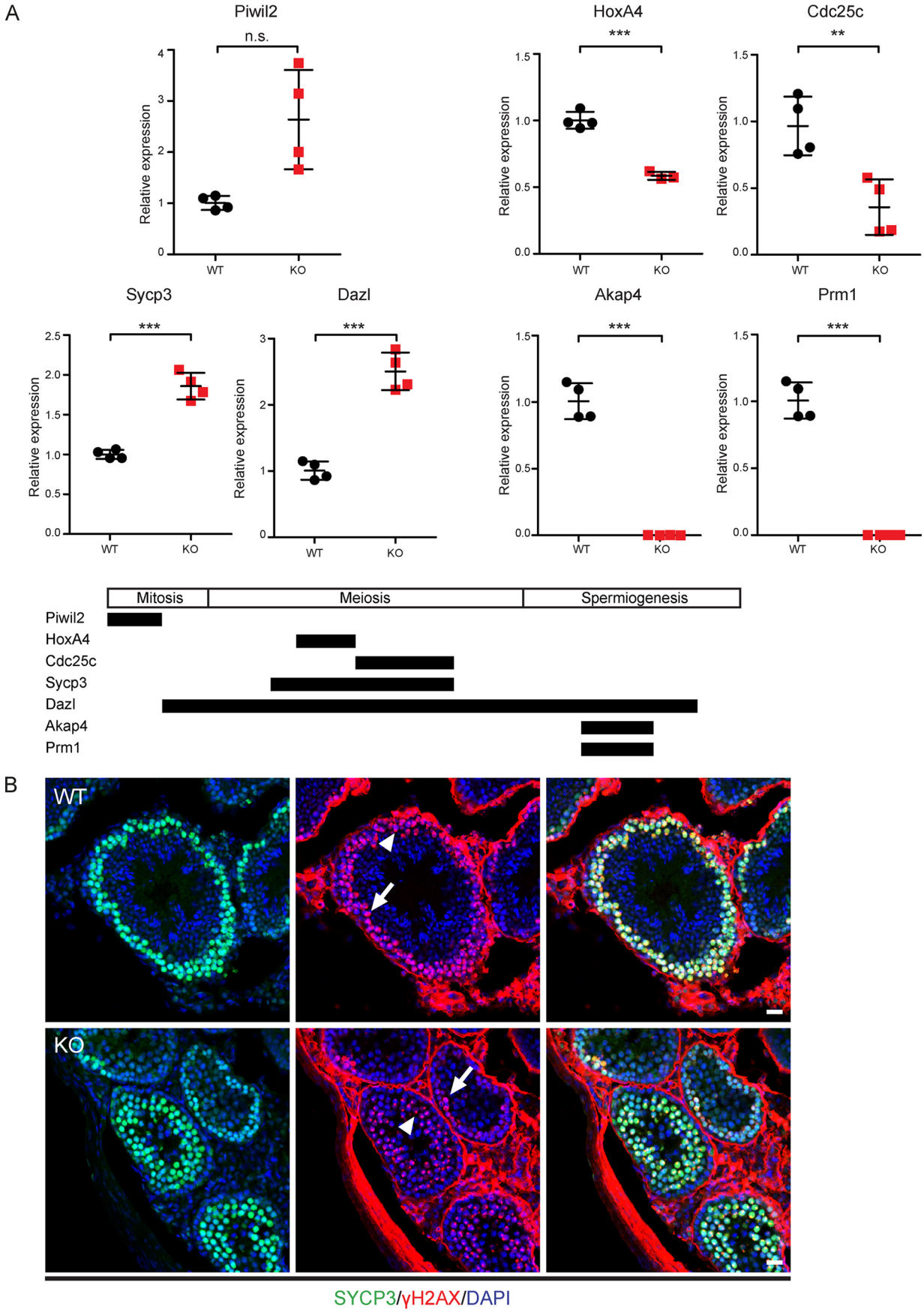
A
Piwil2
n.s.
HoxA4
***
Cdc25c
**
Sycp3
***
Dazl
***
Akap4
***
Prm1
***
Relative expression
WT
KO
Mitosis
Meiosis
Spermiogenesis
Piwil2
HoxA4
Cdc25c
Sycp3
Dazl
Akap4
Prm1
B
WT
KO
SYCP3/γH2AX/DAPI

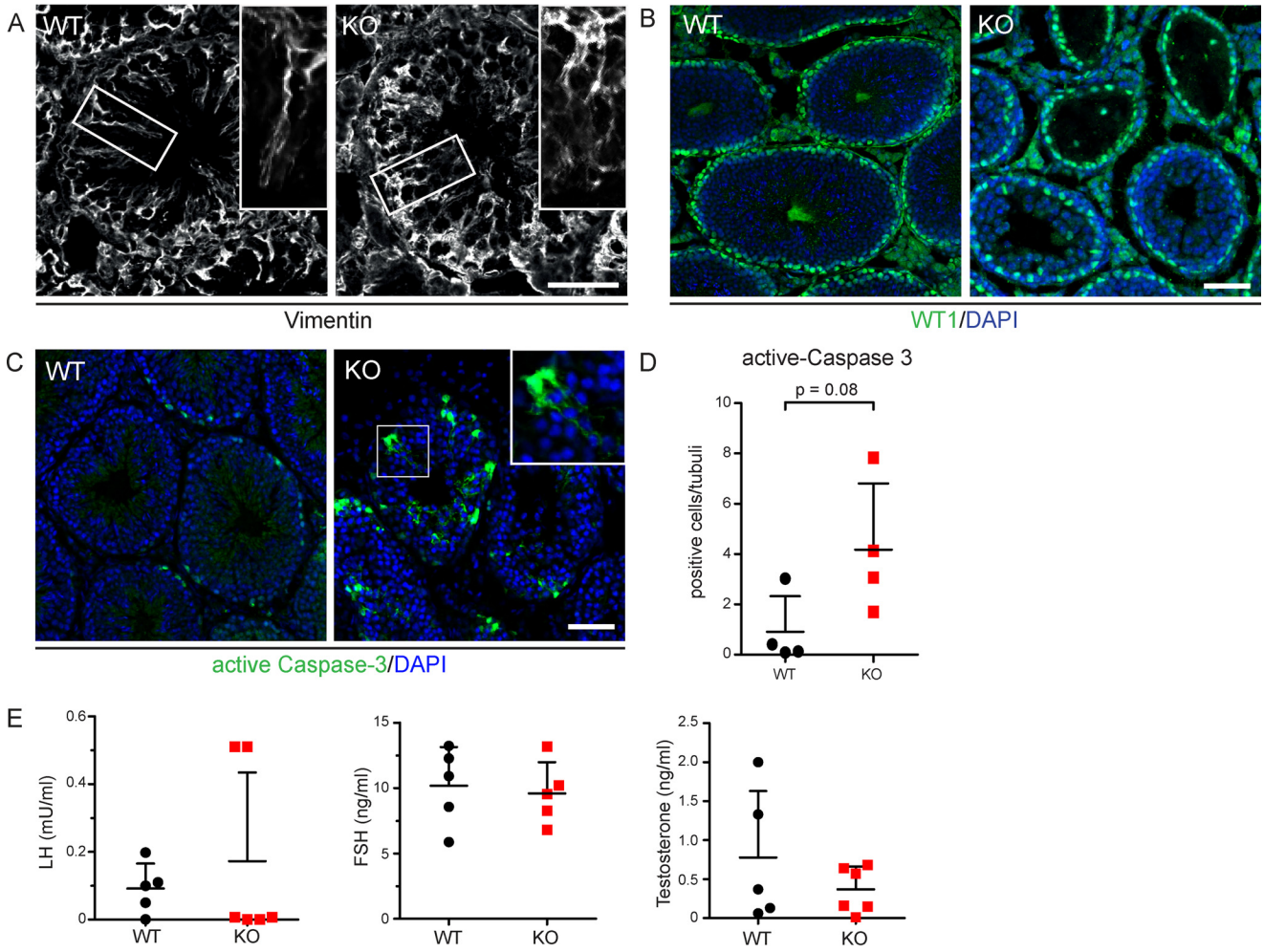

Figure 3. Loss of BT-IgSF influences the overall morphology of Sertoli cells but not the hormonal balance. *A*, immunofluorescence staining against vimentin, a cytoplasmic Sertoli cell marker. Note the irregular and disturbed cytoplasmic arms of Sertoli cells in BT-IgSF knock-out mice. *Scale bar*, 50 μm. *B*, immunofluorescence staining against WT1, a Sertoli cell marker located in the nucleus, shows normal Sertoli cell localization in tubuli and number in knock-out mice. *Scale bar*, 50 μm. *C*, immunofluorescence staining against active caspase-3, a marker for apoptosis, shows slightly more apoptotic cells in knock-out testes, especially in Sertoli cells (*inset*). *Scale bar*, 50 μm. *D*, quantitation of apoptotic cells per tubuli. No significant difference between knock-out and wild-type testes was observed ($n = 5$ per group). The data are shown as means ± S.D. ($p = 0.08$; *t* test). *E*, no hormonal changes in LH ($p = 0.78$), FSH ($p = 0.69$), and testosterone ($p = 0.79$) levels were detected in BT-IgSF knock-out males, compared with wild-type (WT, $n = 5$; KO, $n = 6$). The data are shown as means ± S.D. (differences were not significant; Mann–Whitney test).

that was significantly lower compared with vehicle treated animals (Fig. 6*B*). In histological sections, vehicle-treated animals had normal testis morphology (Fig. 6*A*), whereas tamoxifen-treated animals showed testis with seminiferi tubuli resembling the morphology of BT-IgSF from non-conditional knockouts. They showed vacuolation, the lack of sperms and cytoplasmic extension of Sertoli cells (Fig. 6*A*). However, a number of normal seminiferi tubuli were also detected.

Consistently, by flow cytometry we detected significantly less 1C (haploid, 23 chromatids) cells in tamoxifen-treated animals than in vehicle-treated controls. We measured a higher percentage of cells with 2C (haploid, 23 chromosomes) and 4C (diploid, 46 chromosomes), suggesting that more cells enter meiosis (Fig. 6, *C* and *D*). The analysis of knock-out efficiency by qRT-PCR showed that the BT-IgSF at the mRNA level expression was reduced by ~50%, which is obviously not sufficient to maintain proper spermatogenesis (Fig. 6*E*). In these conditional mutants Cx43 expression was up-regulated as observed in the non-conditional knock-out, which again was accompanied with localization throughout the tubule. The reduced expression of Prm1 again confirms the reduction of sperms (Fig. 6*E*, *right panel*).

Discussion

Spermatogenesis depends on intensive cross-talks between germ and Sertoli cells and intact cell–cell contacts. The dis-

Figure 2. The lack of BT-IgSF leads to spermatogenic arrest. *A*, qRT-PCR analysis of meiotic genes from testis lysates of wild-type and BT-IgSF knock-out mice. Gene expression was normalized to Rplp0 and indicated as fold change to WT. Piwil2 was used as a marker for stem cells, HoxA4 and Cdc25c were used as markers for mid-pachytene stage and late pachytene stage, for overall pachytene stage SycP3 was used, for meiotic germ cells Dazl was used, and for the postmeiotic haploid stages Prm1 and Akap4 were used ($n = 4$ per genotype). The data are shown as means ± S.D. *n.s.*, not significant; **, $p < 0.01$; ***, $p < 0.001$ (*t* test). The scheme illustrates the pattern of expression of genes investigated during germ maturation. *B*, immunofluorescence staining of cryosections against γH2AX and SYCP3. *Arrows*, leptotene stage; *arrowheads*, diplotene stage; *scale bar*, 20 μm.

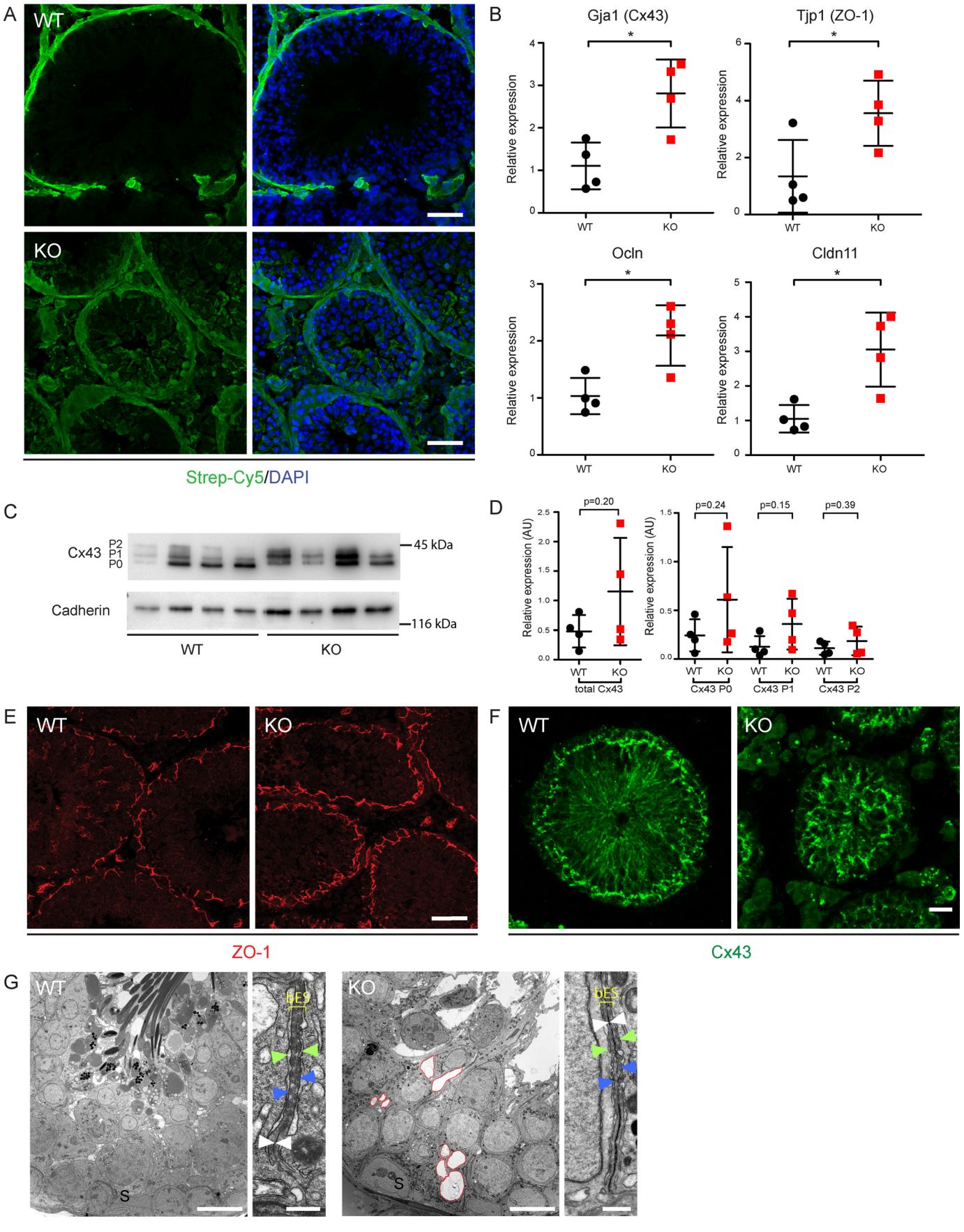
A
WT
KO
Strep-Cy5/DAPI
B
Gja1 (Cx43)
Tjp1 (ZO-1)
Ocln
Cldn11
Relative expression
WT
KO
C
Cx43
P2
P1
P0
45 kDa
Cadherin
116 kDa
WT
KO
D
p=0.20
p=0.24
p=0.15
p=0.39
Relative expression (AU)
total Cx43
Cx43 P0
Cx43 P1
Cx43 P2
E
WT
KO
ZO-1
F
WT
KO
Cx43
G
WT
KO
bES
S

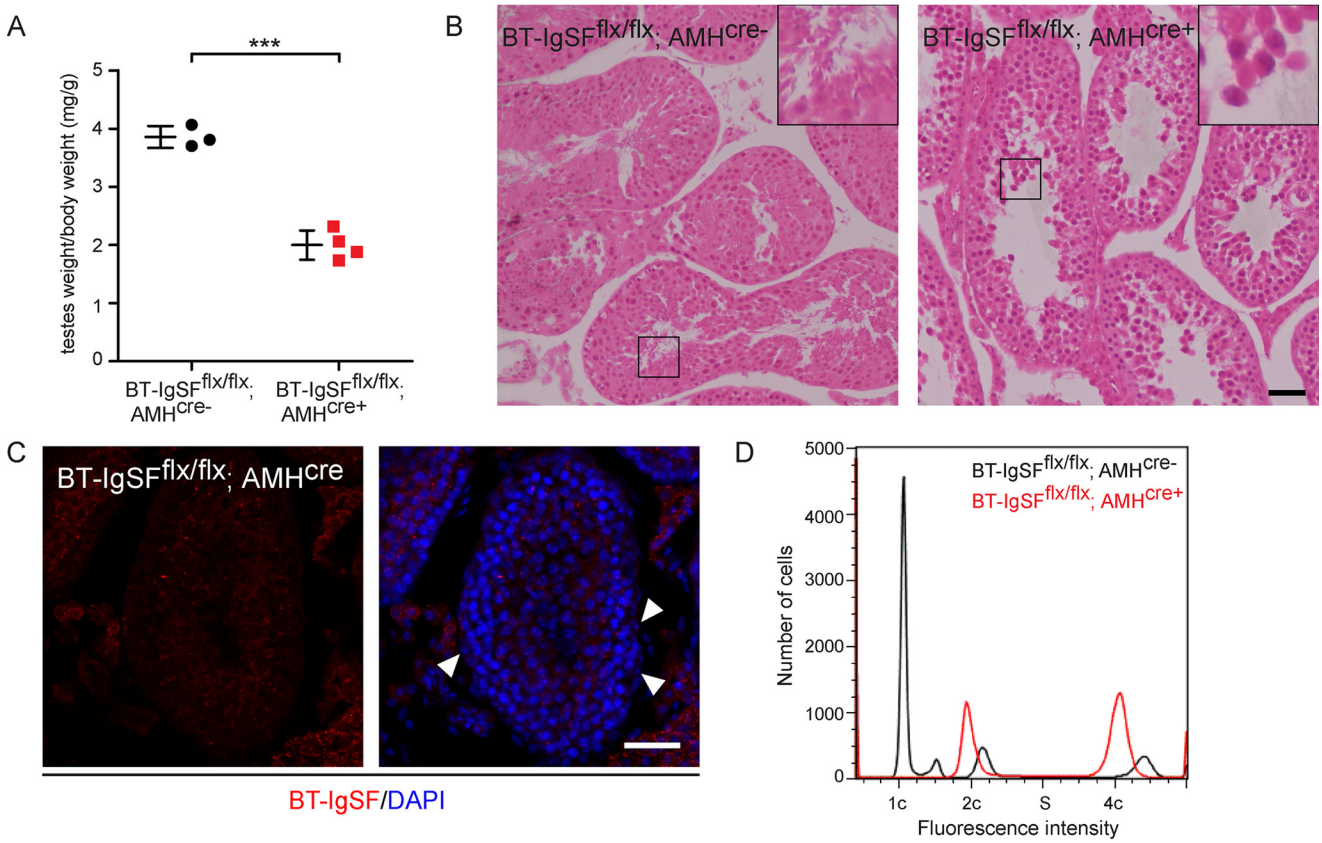

Figure 5. Infertility is due to the absence of BT-IgSF in Sertoli cells. *A*, AMH-cKO testes show a significantly decreased wet weight compared with control animals ($n = 3$ for control and $n = 4$ for AMH-cKO). The data are shown as means ± S. D. ***, $p < 0.001$ (*t* test). *B*, H&E stainings of methacrylate-sections show atrophic testes of AMH-cKO mice compared with wild type. *Scale bar*, 50 μm. *C*, immunofluorescence staining against BT-IgSF in AMH-cKO showing the absence of BT-IgSF signal in Sertoli cells (*arrowhead*). *Scale bar*, 50 μm. *D*, flow cytometric analysis of testis cells, stained with DAPI, shows the lack of haploid chromatin containing cells in AMH-conditional knockouts (*red*) compared with BT-IgSF$^{flx/flx}$ control (*black*). *1c*, haploid, 23 chromatids; *2c*, haploid, 23 chromosomes; *S*, S phase; *4c*, diploid, 46 chromosomes.

turbance of such cell junctions through the impairment of cell–cell adhesion disrupts the BTB and leads to infertility. One paradigmatic group of cell adhesion proteins expressed in the testis is the CAR subgroup of IgCAMs comprising CAR, CLMP, and BT-IgSF (27, 28). However, neither CAR nor CLMP have been found to be crucial for maintaining the integrity of the BTB or for male fertility (27, 29), although CAR interacts with JAM-C, which is crucial for fertility (30).

In this study, we showed that another member of the CAR subgroup, BT-IgSF, is also expressed at the BTB close to the Sertoli cell nucleus. The expression of BT-IgSF in Sertoli cells was further confirmed by a Sertoli-specific (AMH^{Cre}) knock-out of BT-IgSF. AMH is only expressed in fetal Sertoli cells in males, enabling a Sertoli cell specific knock-out of BT-IgSF (31). Furthermore, a co-localization of BT-IgSF with Espin, a marker for the ES, was observed.

Stainings with antibodies against BT-IgSF showed signals at the basal side at Sertoli cells but also at the membrane of cells located at the adluminal side. Whether this labeling is restricted to the cytoplasmic arms of Sertoli cells stretching to the lumen or is located at the membrane of germ cells cannot be definitely decided. However, there is strong evidence that BT-IgSF functions primarily in Sertoli cells. The BT-IgSF expression is strongest at the basal side at Sertoli cells. In the absence of BT-IgSF, we observed defects in the BTB, which is *in vivo* only constituted of cell junctions between Sertoli–Sertoli cells and not between Sertoli–germ cells or germ–germ cells (32). Furthermore, the Sertoli cell–specific knock-out of BT-IgSF shows exact the same phenotype as in the global knock-out, leading to our conclusion that BT-IgSF is mainly important for proper Sertoli cell function. Whether BT-IgSF is also on germ cells might be determined by immunolabeled electron microscopy,

Figure 4. BT-IgSF loss leads to an impaired BTB and up-regulation of transcripts encoding BTB proteins. *A*, *in vivo* biotin assay to test the functionality of the BTB. Biotin distribution is visualized by streptavidin-Cy5 staining; knock-out testis show distribution through all layers of the seminiferous epithelium, indicating an impaired BTB ($n = 3$ per genotype). *Scale bar*, 50 μm. *B*, analysis of BTB gene expression by qRT-PCR; Gja1, Tjp1, Occludin, and Cldn11 are up-regulated in knock-out testes ($n = 4$ per group). The data are shown as means ± S.D. *, $p < 0.05$ (*t* test). *C* and *D*, protein expression of Cx43. *P0*, unphosphorylated; *P1* and *P2*, phosphorylated forms. Anti-pan-cadherin was used as a loading control. Three independent blots were analyzed that showed no significant differences between WT and KO (*t* test). The data are shown as means ± S.D. *E*, immunofluorescence staining against ZO-1, a tight junction protein of the BTB; note the slightly less organized localization of ZO-1 in knock-out testis. *Scale bar*, 50 μm. *F*, immunofluorescence staining against Cx43, a gap junction protein of the BTB; note the diffuse localization of Cx43 in knock-out testis. *Scale bar*, 20 μm. *G*, electron microscopy of adult testis. At higher magnifications, no differences between WT and KO were observed in the basal ES, typified by the actin filament bundles (*blue arrowheads*) sandwiched between cisternae of the endoplasmic reticulum (*green arrowheads*) and the plasma membranes of two Sertoli cells, tight junction (*white arrowheads*) co-existing with the basal ES. *Red outlines*, vacuoles; *S*, Sertoli cells; *scale bars*, 10 μm for *left panel* (WT and KO) and 500 nm for *right panel* (WT and KO).

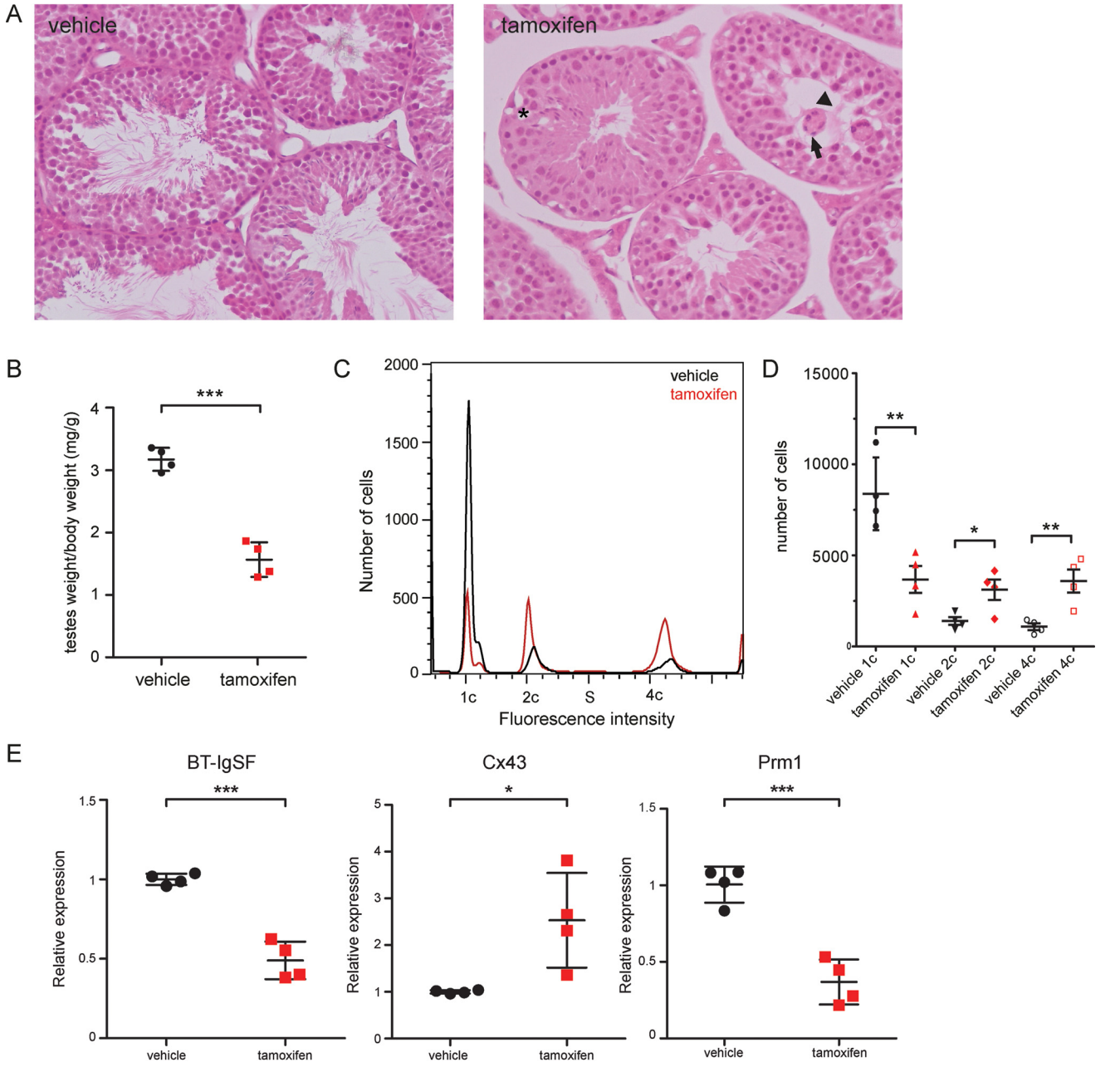

Figure 6. Loss of BT-IgSF in adulthood also affects spermatogenesis. *A*, H&E stainings of methacrylate-sections show atrophic testes of BT-IgSF$^{flx/flx}$;Rosa26CreERT2 mice treated with tamoxifen compared with vehicle control. *B*, BT-IgSF$^{flx/flx}$;Rosa26CreERT2 testis treated with tamoxifen show a significantly decreased wet weight compared with vehicle treated animals ($n = 4$ for vehicle and $n = 4$ for tamoxifen). The data are shown as means ± S.D. ***, $p < 0.001$ (*t* test). *C* and *D*, flow cytometric analysis of testis cells, stained with DAPI, shows the reduction of haploid chromatin containing cells by tamoxifen treatment of BT-IgSF$^{flx/flx}$;Rosa26CreERT2 (*red*) compared with vehicle control (*black*) and the increase in 2C and 4C cells. *1c*, haploid, 23 chromatids; *2c*, haploid, 23 chromosomes; *S*, S phase; *4c*, diploid, 46 chromosomes. *E*, analysis of expression of Cx43 and Prm1 transcripts by qRT-PCR. BT-IgSF expression is reduced by ~50% in tamoxifen-treated testes. Gja1 (Cx43) is up-regulated in tamoxifen treated testes; Prm1, a marker for spermatids and sperm, is significantly reduced ($n = 4$ per group). The data are shown as means ± S.D. *, $p < 0.05$; **, $p < 0.01$; ***, $p < 0.001$ (*t* test).

for which, however, appropriate antibodies are currently not available.

Loss of BT-IgSF leads to atrophic testes, an arrest of spermatogenesis and male infertility. The testis size of BT-IgSF knock-out mice is drastically reduced compared with control mice which is due to a lack of sperms and spermatids, vacuolation, and misorganized cytoplasmic arms of Sertoli cells. Identical results were obtained with a Sertoli cell–specific knock-out of BT-IgSF (AMH^{Cre}). These males also exhibit smaller testis with no haploid spermatids and are infertile, confirming that the expression of BT-IgSF in Sertoli cells is essential for male fertility in mice. A similar phenotype was also observed in other mutants like the TAp73 knock-out mouse (33). Analyses of meiosis I–specific genes and immunofluorescence stainings against SYCP3 and γH2AX did not show major changes at meiosis I in the absence of BT-IgSF. Quantitative PCR of meiosis-related genes demonstrated a normal meiosis I from leptotene to diplotene. Consistently, secondary spermatocytes with the chromosomal status of 2C and 1n (haploid chromosome set) were present, whereas no 1C-containing cells, sperm, and sper-

matids were detected in BT-IgSF knock-out males (Fig. 1*H*). Furthermore we observed that all meiotic cells are positive for γH2AX, indicating that no cell enters meiosis II. Therefore, spermatogenesis arrest must occur after meiosis I. However, the investigation of meiosis II is complicated because of its strong similarity to mitosis. Further studies might clarify whether meiosis II is initiated all.

We showed that the arrest is probably due to an impaired BTB accompanying with changes in the localization of BTB proteins. In the *in vivo* biotin assay, the biotin tracer was detected inside the seminiferi tubuli, indicative for a defect BTB. Transcripts of the major tight junction and gap junction proteins of the BTB like ZO-1, Occludin, and Cx43 were upregulated in BT-IgSF knock-out testes, and importantly, a mislocalization of Cx43 and ZO-1 was observed in the Sertoli cells. However, Sertoli cell–Sertoli cell junctions were unaffected when examined by electron microscopy.

Normally, Cx43 is predominantly expressed in Sertoli cells at the BTB. In contrast to wild-type, BT-IgSF knock-out animals exhibit a disturbed CX43 expression pattern. Cx43 is not only expressed at the basal BTB barrier but is irregularly distributed and also found in adluminal compartments. Similar findings were also detected in *Fads2* (fatty acid desaturase 2) knock-out mice (34). The loss of FADS2 leads to smaller testes; to mislocalization of several BTB proteins like Cx43, Occludin, and ZO-1; and to a disrupted BTB, as observed in the BT-IgSF mutant mice. Cx43 is the predominant connexin in the testis, and its importance for male fertility has been shown by several studies. The global knock-out of Cx43 leads to death soon after birth because of heart defects. Also at early developmental stages Cx43 has an impact on fertility. From embryonic day 11.5 on, the testes of Cx43 knockouts are smaller compared with wild-type testes, which is mainly due to germ cell deficiency (35, 36). To study the function of Cx43 in adult males, a Sertoli cell–specific Cx43 knock-out was analyzed (13). Sertoli cells exhibited vacuolation and an arrest of spermatogenesis at spermatogonia, leading to male infertility. In electron microscopic images, no changes were detected in the BTB, but these knockout animals revealed an overexpression of BTB proteins, and their localization in the tubuli was more diffuse (37); these findings are similar to the phenotype described here for BT-IgSF.

A number of studies have shown that knock-out of BTB proteins including Claudin11, ZO-2, and Occludin lead to infertility (10–12, 38). The phenotypes are very similar to those observed in BT-IgSF knock-out males. Claudin11 knock-out males have smaller testes, no spermatids, and Sertoli cell aggregates, and apoptosis of germ cells occurs (38). The BT-IgSF knock-out also showed smaller testes, no spermatids, and multinucleated cell aggregates in the lumen. However, no significant increase in apoptosis could be shown for BT-IgSF–deficient males. ZO-2 knock-out males have an impaired BTB, and Occludin knockouts revealed an atrophic testis in old males. The defects in the BTB of Occludin knock-out males are comparable with the impaired BTB of BT-IgSF– deficient animals. Taken together, the cell adhesion molecule BT-IgSF is expressed at the BTB and is important for its integrity.

Whether the increase in expression of the BTB proteins Cx43, ZO-1, Occludin, and Claudin11 is due to a direct effect of BT-IgSF loss or just a compensation of the loss of one cell adhesion molecule remains to be determined. It is also interesting to determine whether the loss of BT-IgSF directly leads to an impaired BTB or whether altered gap junction activity is the major reason for an impaired BTB. Cx43 phosphorylation is important to regulate gap junction function and the localization of Cx43 molecules (39). We observed a tendency to an increased Cx43 phosphorylation that might change the gap junction position and activity.

Interestingly, it is known that ZO-1 interacts with Cx43 through the second PDZ domain of ZO-1 (40). An interaction between ZO-1 and BT-IgSF is conceivable because a strong co-localization was detected (Fig. 1*F*). Also, a co-localization of BT-IgSF and Cx43 was observed, enabling a close proximity and a possible indirect interaction through ZO-1. Furthermore, an interaction of ZO-1 with the cytoplasmic segments of the closely related cell adhesion proteins CLMP and CAR have been published (27, 41, 42). Therefore, it seems reasonable to conclude that also BT-IgSF with its C-terminal located PDZ-binding motif interacts with one of the PDZ domains of ZO-1 and therefore also indirectly with Cx43. With this, a complex between BT-IgSF, ZO-1, and Cx43 might be formed in Sertoli cells.

It is of note that changes in Cx43 expression also lead to infertility in humans. In patients with secretory azoospermia Cx43 expression was shown to be reduced (43).

Because in the absence of BT-IgSF the ultrastructure of the BTB appears normal in electron microscopic images, we conclude that BT-IgSF might be essential for a functional BTB and appears to interfere with barrier dynamics including the localization of connexin43 and the expression of junctional proteins. It would be of interest to analyze whether also BT-IgSF expression is changed in patients with azoospermia, especially in patients with a spermatogenic arrest at the level of secondary spermatocytes. Further investigations on the mechanistic regulation of BT-IgSF might help to better understand unknown causes of human male infertility.

Experimental procedures

Mouse strains

The B6-Igsf11$^{tm1e(KOMP)Wtsi}$ mouse strain used for this research project was generated from targeted ES Cells (JM8.N4) obtained from the Knock-Out Mouse Project (KOMP) Repository (clone EPD0297_2_B07). ES cells were injected into C57BL/6N blastocysts at the transgenic core facility of the Max Delbrück Center. Founders were crossed with C57BL/6N. To remove the neo cassette, mice were bread to 129S1-Hprt$^{tm1(cre)Mnn}$ mice (44) and further backcrossed with C57/Bl6. Correct insertion of the construct was tested with a 5′ probe amplified with the primers 5′-GGGGGATCCAGGTTT-GCAGTGAGGAGAATCA-3′ and 5′-GGACGTCAGAAAC-AGTCAAGACAGCGGG-3′. Absence of BT-IgSF protein was tested by immunofluorescence stainings and Western blotting (Fig. S1). The resulting animals are termed BT-IgSF KO mice in this study.

For the BT-IgSF^{flx} mice (B6-Igsf11$^{tm1a(KOMP)Wtsi/Fgr}$), sperm for the *in vitro* fertilization was derived from mice generated by KOMP Repository and the Mouse Biology Program at the Univer-

sity California Davis with ES from the Welcome Trust Sanger Institute (clone EPD0297_2_A07). The IVF was done by the transgenic core facility of the Max Delbrück Center. The resulting mice were crossed to Tg(ACTFLPe)9205Dym (45), to remove the trapping cassette, and to obtain a conditional allele. These animals are called BT-IgSF^{flx} (B6-Igsf11$^{tm1c(KOMP)Wtsi/Fgr}$).

To obtain a Sertoli cell–specific BT-IgSF knock-out, BT-IgSF$^{flx/flx}$ mice were bred to B6-Tg(Amh-cre)8815Reb/J mice (National Institute for Agronomic Research) (30). The mice are designated AMH-conditional KO (BT-IgSF$^{flx/flx}$; AMH^{Cre}).

To obtain a conditional, tamoxifen-inducible BT-IgSF knock-out mouse, a Rosa26^{CreERT2} mouse line (B6.129-Gt(ROSA)26Sortm1(cre/ERT2)Tyj/J, Jackson Stock 008463) was crossed to BT-IgSF^{flx} mice, resulting in animals called BT-IgSF$^{flx/flx}$; Rosa26^{CreERT2}. Tamoxifen treatments were performed at an age of 8–12 weeks with 1.5 mg of tamoxifen (Sigma; T5638) dissolved in corn oil (Sigma; C8267) on 5 consecutive days i.p. Controls were treated with corn oil (vehicle) only. The experiment was terminated 10 weeks after the first tamoxifen administration.

The animals were housed on a 12/12-h light/dark cycle with free access to food and water. The animal procedures were performed according to the guidelines from directive 2010/63/EU of the European Parliament on the protection of animals used for scientific purposes. All experiments were approved by the local authorities of Berlin (LaGeSO) (numbers T0313/97, X 9007/16, O 0038/08, G 0188/16, S0032/03, 0143/07, and H0237/04). The mice investigated were 8–12 weeks old. Littermates served as controls.

Genotyping

Genotyping was performed by PCR amplification of genomic DNA isolated from tail or ear punches. For the BT-IgSF KO animals, primers P1 (5′-ACATGCACAGGAAGGTCCTC-3′) and P2 (5′-TCATTCGAGCAATGCCTTTT-3′) result in a fragment of 197 bp in the wild-type condition and primer P1 and P3 (5′-CTTCTGATGAGGTGGTCCCA-3′) in a fragment of 343 bp in the knock-out condition. The floxed allele of the BT-IgSF$^{flx/flx}$ mouse was genotyped by primer P1 and P2, which will lead to fragments of 197 bp in the wild-type and of 379 bp in the floxed condition, respectively. The presence of the Cre allele was tested with the primers P4 (5′-GAACGCACTGATTTCGACCA-3′) and P5 (5′-AACCAGCGTTTTCGTTCTGC-3′) and will result in a fragment of 200 bp.

Flow cytometry

50 mg of decapsulated testis were minced in a solution containing 0.1 M citric acid and 0.5% Tween 20 and stained with 1.75 μg/ml DAPI. The filtered cell suspension was measured and analyzed on a Canto II (BD Biosciences). The data were analyzed with FlowJo Software (Treestar).

Histology, testis weight, immunohistochemistry, and generation of anti-BT-IgSF

For H&E stainings and immunofluorescence stainings, transcardial perfusion with 4% PFA in PBS was performed. Testes were postfixed for H&E stainings overnight at 4 °C with 4% PFA in PBS. For immunofluorescence staining against active caspase-3, only 1% PFA in PBS was used as fixative. Gross morphology analysis of testes was performed on 5-μm methacrylate slices (Technovit 7100) stained with H&E. Body weight and wet testis weight were measured directly after sacrificing the mice. Rb95 to mouse BT-IgSF was generated by injecting five times of 50 μg of a fusion protein composed of the extracellular part of mBT-IgSF (amino acid residues 23–239, LEV . . . PRS) fused to the Fc fragment of human IgG1 supplemented with Freund's adjuvant into rabbits at fortnightly intervals. Rb113 was generated using the same protocol and the same fusion protein; however, it was denatured in 20% SDS and 20 mM DTT as immunogen as used for the production of Rb95 (see above). The IgG fractions were purified by protein A (GE Healthcare) affinity chromatography.

Antibody stainings were performed on 16-μm paraformaldehyde-fixed cryosections. The following primary and fluorophore-conjugated secondary antibodies were applied: rabbit anti-BT-IgSF Rb95 (1 μg/ml), rabbit anti-vimentin (abcam, 92547, 1:300), rabbit anti-WT1 (abcam, ab15249, 1:300), rabbit anti-Cx43 (Cell Signaling, 3512, 1:100), mouse anti-Cx43 (B&D, 610061, 1:250), mouse anti-ZO-1 (Invitrogen, 339100, 5 μg/ml), rabbit anti-ZO-1 (Invitrogen, 40-2200, 1:100), rabbit anti-ZO-2 (Cell Signaling, 2847S, 1:50), rabbit anti-SYCP3 (abcam, 15093, 1:500), mouse anti-γH2AX (Novus Biologicals, NB100–74435, 3 μg/ml), and mouse anti-Espin (B&D, 611656, 1:200). Secondary antibodies were used at 1:800 and DAPI at 1 μg/ml. Goat anti-rabbit Cy3 (Jackson ImmunoResearch, 111-165-144), goat anti-rabbit A488 (Invitrogen, A11034), goat anti-mouse A488 (Invitrogen, A11029). For WT1 staining an antigen-retrieval protocol with citrate buffer (10 mM sodium citrate buffer, 0.05% Tween 20, pH 6.0) was performed. Blocking was done at room temperature for 1 h with 3% goat serum, 1% BSA in PBS with 0.1% Triton X-100. Primary antibodies were incubated overnight at 4 °C, and secondary antibodies were incubated at room temperature for 2 h.

Microscopic images were obtained at room temperature by confocal imaging using a Carl Zeiss LSM 700 laser scanning microscope equipped with ZEN 2011 software and the following lenses: a Plan-Neofluar 20×/0.30 NA objective or a Plan-Achromat 63×/1.40 NA oil objective (all from Carl Zeiss MicroImaging, GmbH). Images were imported into Photoshop CS5 (Adobe) for uniform adjustment of contrast and brightness. The figures were assembled using Illustrator CS5 (Adobe).

Western blotting

Testes were decapsulated and homogenized, and membranes were enriched by centrifugation followed by stripping off peripheral proteins in 0.1 M diethylamine at pH 11.5. For Western blotting, the following antibodies were used: Rb113 (0.75 μg/ml), rabbit anti-Cx43 (Cell Signaling 3512, 1:1000), and, as a loading control, rabbit anti-pan-Cadherin (Sigma, C3678, 1:1000). Analyses of three independent blots were done with Quantity One (Bio-Rad).

Apoptosis

Apoptosis analysis was done on 15-μm cryosections stained against active caspase-3 (Promega, G7481, 1:400). Positive cells per

Table 1
Primer used for qRT-PCR analysis

Gene	Forward primer (5′ → 3′)	Reverse primer (5′ → 3′)	Amplicon size
			bp
Rplp0	GGACCCGAGAAGACCTCCTT	GCACATCACTCAGAATTTCAATGG	85
BT-IgSF	TGCACTAATTTCAGGGGCGT	GCCAGAGAAAGACTGGCGTA	268
Gja1 (Cx43)	GAACACGGCAAGGTGAAGAT	GACGTGAGAGGAAGCAGTCC	187
Tjp1 (ZO-1)	GTTTAGGAGCACCAAGTGC	TCCTGTACACCTTTGCTGG	96
Ocln	TGGCTGCTGCTGATGAATA	CATCCT CTTGATCTGCGATAAT	116
Cldn11	TCCTTATTCTGCTGGCTCTC	AGCTCACGATGGTGATCTC	84
Piwil2	GCACAGTCCACGTGGTGGAAA	TCCATAGTCAGGACCGGAGGG	681
HoxA4	CACAAAATTCCACCTGCTCACA	CATCGGTATCTGGCCATGGT	113
Cdc25c	GGCCACGTAGATGCAATTTTAAC	GCGAAGACTCCACAGAATGACA	76
Hist1h1c	AGAAGCCTAAGAAGGCGACTG	TCTTGGCCACTTTCTTGGTC	111
Sycp3	AGCCAGTAACCAGAAAATTGAGC	CCACTGCTGCAACACATTCATA	105
Dazl	AATGTTCAGTTCATGATGCTGCTC	TGTATGCTTCGGTCCACAGACT	73
Akap4	GACTGGTCTTGTTTTTCAGTGTCC	TGCTGGTTCCAGGTCAGAAG	93
Prm1	CACAAAATTCCACCTGCTCACA	CATCGGTATCTGGCCATGGT	103

tubuli were counted (40–50 tubuli per section, $n = 4$ per genotype).

qRT-PCR

Total RNA was isolated from decapsulated testis using the RNeasy mini kit (Qiagen), including an on-column DNase I digestion. RNA yield was measured by Nanodrop 1000 (Nanodrop). RNA was transcribed by SuperScript II (Invitrogen) using oligo(dT) primers. The quantitative real-time PCR was performed on a 7500 fast real-time PCR system (Applied Biosystems) with GoTaq quantitative PCR Master Mix (Promega). Rplp0 was used as a housekeeping gene. Technical triplicates were performed with $n = 4$ testes per genotype. Applied primers are listed in Table 1.

Biotin in vivo assay

The biotin *in vivo* assay was used to examine the integrity of the blood–testis barrier (25). 50 μl of 10 mg/ml EZ-Link Sulfo-NHS-LC-Biotin (Pierce) freshly diluted in PBS containing 1 mM $CaCl_2$ was injected per testis of anesthetized mice. The neighboring testis was injected with 50 μl of 1 mM $CaCl_2$ in PBS and served as a control. After 30 min, the animals were euthanized, and their testes were immediately frozen. Cryosections were stained with Strep-Cy5 (1:600) and 1 μg/ml DAPI.

Electron microscopy

The mice were perfused with 2% formaldehyde, 2.5% glutaraldehyde in 0.1 M phosphate buffer, and the testes were removed, cut in two halves after 2 h, and further fixed for 24 h in the same fixative. Samples were postfixed in 1% osmium tetroxide, 1.5% potassium ferrocyanide in water for 5 h. Following washing with phosphate buffer, the samples were stained with 1% tannic acid in phosphate buffer for 5 h, dehydrated through a graded series of ethanol, and embedded in Poly/Bed 812 (Polysciences, Inc., Eppelheim, Germany). Ultrathin sections were stained with uranyl acetate and lead citrate and examined with a FEI Morgagni electron microscope and the iTEM software (EMSIS GmbH, Münster, Germany).

Hormone status

Serum of animals was analyzed by Laboklin (Bad Kissingen, Germany). FSH and testosterone were measured with a mouse-specific ELISA and LH with a mouse-specific sandwich ELISA (LifeSPan BioSciences Inc., Seattle, WA).

Statistical analysis

Statistical analysis was performed with Excel (Microsoft) and Prism5 (GraphPad). Normality was tested with Shapiro–Wilk normality test. Significance was determined by using the unpaired two-tailed Student's t test, the one-way analysis of variance, or the Mann–Whitney test. Significance was assumed for $p < 0.05$ (*, $p < 0.05$; **, $p < 0.01$; ***, $p < 0.001$; n.s., not significant).

Author contributions—L. P. and F. G. R. conceptualization; L. P. validation; L. P. and B. P. investigation; L. P. visualization; L. P. and B. P. methodology; L. P. and F. G. R. writing-original draft; L. P. and F. G. R. writing-review and editing; F.G.R. supervision; F. G. R. funding acquisition; F. G. R. project administration.

Acknowledgments—We thank Anne Banerjee, Maria Steinecker, and Christina Schiel for technical assistance and Karola Bach for mouse breeding. We also acknowledge Dr. Karin Müller (Leibniz Institute for Zoo and Wildlife Research, Berlin, Germany) and Andreas Pelz (Charité, Berlin, Germany) for flow cytometry experiments and critical reading of the manuscript. We thank the transgenic core facility of the Max Delbrück Center for blastocyst injections and sperm rederivation. The ES cells and sperm used for this research project were generated by the trans-NIH KOMP and obtained from the KOMP Repository (www.komp.org).[3] *We thank Dr. Thomas Jentsch (Max Delbrück Center and FMP, Berlin) and Dr. Florian Guillou (INRA, Paris) for providing* AMH^{Cre} *mice and Karina Oberheide and Corinna Göppner (both from the Max Delbrück Center) for discussion. We thank Dr. Spagnoli (Max Delbrück Center) for providing* $Rosa26^{CreERT2}$ *mice. We acknowledge support from Velocigene at Regeneron Inc. (supported by National Institutes of Health Grant U01HG004085) and the CSD Consortium (supported by National Institutes of Health Grant U01HG004080), which funded the generation of gene-targeted ES cells for 8500 genes in the KOMP Program. Also, the archiving and distribution by the KOMP Repository at UC Davis and CHORI were supported by National Institutes of Health Grant U42RR024244.*

[3] Please note that the JBC is not responsible for the long-term archiving and maintenance of this site or any other third party hosted site.

References

1. Suzu, S., Hayashi, Y., Harumi, T., Nomaguchi, K., Yamada, M., Hayasawa, H., and Motoyoshi, K. (2002) Molecular cloning of a novel immunoglobulin superfamily gene preferentially expressed by brain and testis. *Biochem. Biophys. Res. Commun.* **296,** 1215–1221
2. Katoh, M., and Katoh, M. (2003) IGSF11 gene, frequently up-regulated in intestinal-type gastric cancer, encodes adhesion molecule homologous to CXADR, FLJ22415 and ESAM. *Int. J. Oncol.* **23,** 525–531
3. Matthäus, C., Langhorst, H., Schütz, L., Jüttner, R., and Rathjen, F. G. (2017) Cell–cell communication mediated by the CAR subgroup of immunoglobulin cell adhesion molecules in health and disease. *Mol. Cell. Neurosci.* **81,** 32–40
4. Eom, D. S., Inoue, S., Patterson, L. B., Gordon, T. N., Slingwine, R., Kondo, S., Watanabe, M., and Parichy, D. M. (2012) Melanophore migration and survival during zebrafish adult pigment stripe development require the immunoglobulin superfamily adhesion molecule Igsf11. *PLoS Genet.* **8,** e1002899
5. Harada, H., Suzu, S., Hayashi, Y., and Okada, S. (2005) BT-IgSF, a novel immunoglobulin superfamily protein, functions as a cell adhesion molecule. *J. Cell. Physiol.* **204,** 919–926
6. Jang, S., Oh, D., Lee, Y., Hosy, E., Shin, H., van Riesen, C., Whitcomb, D., Warburton, J. M., Jo, J., Kim, D., Kim, S. G., Um, S. M., Kwon, S.-K., Kim, M.-H., Roh, J. D., *et al.* (2016) Synaptic adhesion molecule IgSF11 regulates synaptic transmission and plasticity. *Nat. Neurosci.* **19,** 84–93
7. Ahi, E. P., and Sefc, K. M. (2017) A gene expression study of dorso-ventrally restricted pigment pattern in adult fins of *Neolamprologus meeli*, an African cichlid species. *PeerJ.* **5,** e2843
8. Mruk, D. D., and Cheng, C. Y. (2012) In search of suitable *in vitro* models to study germ cell movement across the blood–testis barrier. *Spermatogenesis* **2,** 6–10
9. Xiao, X., Mruk, D. D., Wong, C. K., and Cheng, C. Y. (2014) Germ cell transport across the seminiferous epithelium during spermatogenesis. *Physiology* (*Bethesda*) **29,** 286–298
10. Gow, A., Southwood, C. M., Li, J. S., Pariali, M., Riordan, G. P., Brodie, S. E., Danias, J., Bronstein, J. M., Kachar, B., and Lazzarini, R. A. (1999) CNS myelin and Sertoli cell tight junction strands are absent in Osp/Claudin-11 null mice. *Cell* **99,** 649–659
11. Saitou, M., Furuse, M., Sasaki, H., Schulzke, J. D., Fromm, M., Takano, H., Noda, T., and Tsukita, S. (2000) Complex phenotype of mice lacking occludin, a component of tight junction strands. *Mol. Biol. Cell.* **11,** 4131–4142
12. Xu, J., Anuar, F., Ali, S. M., Ng, M. Y., Phua, D. C., and Hunziker, W. (2009) Zona occludens-2 is critical for blood–testis barrier integrity and male fertility. *Mol. Biol. Cell.* **20,** 4268–4277
13. Brehm, R., Zeiler, M., Rüttinger, C., Herde, K., Kibschull, M., Winterhager, E., Willecke, K., Guillou, F., Lécureuil, C., Steger, K., Konrad, L., Biermann, K., Failing, K., and Bergmann, M. (2007) A Sertoli cell–specific knockout of connexin43 prevents initiation of spermatogenesis. *Am. J. Pathol.* **171,** 19–31
14. Sridharan, S., Simon, L., Meling, D. D., Cyr, D. G., Gutstein, D. E., Fishman, G. I., Guillou, F., and Cooke, P. S. (2007) Proliferation of adult Sertoli cells following conditional knockout of the gap junctional protein GJA1 (connexin 43) in mice. *Biol. Reprod.* **76,** 804–812
15. Jiang, X.-H., Bukhari, I., Zheng, W., Yin, S., Wang, Z., Cooke, H. J., and Shi, Q.-H. (2014) Blood–testis barrier and spermatogenesis: lessons from genetically-modified mice. *Asian J. Androl.* **16,** 572–580
16. França, L. R., Hess, R. A., Dufour, J. M., Hofmann, M. C., and Griswold, M. D. (2016) The Sertoli cell: one hundred fifty years of beauty and plasticity. *Andrology* **4,** 189–212
17. Yan, H. H., Mruk, D. D., Lee, W. M., and Cheng, C. Y. (2007) Ectoplasmic specialization: a friend or a foe of spermatogenesis? *Bioessays* **29,** 36–48
18. Cheng, C. Y., and Mruk, D. D. (2010) A local autocrine axis in the testes that regulates spermatogenesis. *Nat. Rev. Endocrinol.* **6,** 380–395
19. Lee, J. H., Engel, W., and Nayernia, K. (2006) Stem cell protein Piwil2 modulates expression of murine spermatogonial stem cell expressed genes. *Mol. Reprod. Dev.* **73,** 173–179
20. Luangpraseuth-Prosper, A., Lesueur, E., Jouneau, L., Pailhoux, E., Cotinot, C., and Mandon-Pépin, B. (2015) TOPAZ1, a germ cell specific factor, is essential for male meiotic progression. *Dev. Biol.* **406,** 158–171
21. Silva, C., Wood, J. R., Salvador, L., Zhang, Z., Kostetskii, I., Williams, C. J., and Strauss, J. F., 3rd (2009) Expression profile of male germ cell-associated genes in mouse embryonic stem cell cultures treated with all-*trans* retinoic acid and testosterone. *Mol. Reprod. Dev.* **76,** 11–21
22. Handel, M. A. (2004) The XY body: a specialized meiotic chromatin domain. *Exp. Cell Res.* **296,** 57–63
23. Lammers, J. H., Offenberg, H. H., van Aalderen, M., Vink, A. C., Dietrich, A. J., and Heyting, C. (1994) The gene encoding a major component of the lateral elements of synaptonemal complexes of the rat is related to X-linked lymphocyte-regulated genes. *Mol. Cell. Biol.* **14,** 1137–1146
24. Coquelin, A., and Desjardins, C. (1982) Luteinizing hormone and testosterone secretion in young and old male mice. *Am. J. Physiol.* **243,** E257–E263
25. Meng, J., Holdcraft, R. W., Shima, J. E., Griswold, M. D., and Braun, R. E. (2005) Androgens regulate the permeability of the blood–testis barrier. *Proc. Natl. Acad. Sci. U.S.A.* **102,** 16696–16700
26. Cheng, C. Y., and Mruk, D. D. (2012) The blood–testis barrier and its implications for male contraception. *Pharmacol. Rev.* **64,** 16–64
27. Sze, K.-L., Lee, W. M., and Lui, W.-Y. (2008) Expression of CLMP, a novel tight junction protein, is mediated via the interaction of GATA with the Kruppel family proteins, KLF4 and Sp1, in mouse TM4 Sertoli cells. *J. Cell. Physiol.* **214,** 334–344
28. Wang, C. Q., Mruk, D. D., Lee, W. M., and Cheng, C. Y. (2007) Coxsackie and adenovirus receptor (CAR) is a product of Sertoli and germ cells in rat testes which is localized at the Sertoli-Sertoli and Sertoli-germ cell interface. *Exp. Cell Res.* **313,** 1373–1392
29. Sultana, T., Hou, M., Stukenborg, J.-B., Töhönen, V., Inzunza, J., Chagin, A. S., and Sollerbrant, K. (2014) Mice depleted of CAR display normal spermatogenesis and an intact blood–testis Barrier. *Reproduction* **147,** 875–883
30. Gliki, G., Ebnet, K., Aurrand-Lions, M., Imhof, B. A., and Adams, R. H. (2004) Spermatid differentiation requires the assembly of a cell polarity complex downstream of junctional adhesion molecule-C. *Nature* **431,** 320–324
31. Lécureuil, C., Fontaine, I., Crepieux, P., and Guillou, F. (2002) Sertoli and granulosa cell-specific Cre recombinase activity in transgenic mice. *Genesis* **33,** 114–118
32. Mruk, D. D., and Cheng, C. Y. (2015) The mammalian blood–testis barrier: its biology and regulation. *Endocr. Rev.* **36,** 564–591
33. Holembowski, L., Kramer, D., Riedel, D., Sordella, R., Nemajerova, A., Dobbelstein, M., and Moll, U. M. (2014) TAp73 is essential for germ cell adhesion and maturation in testis. *J. Cell Biol.* **204,** 1173–1190
34. Stoffel, W., Holz, B., Jenke, B., Binczek, E., Günter, R. H., Kiss, C., Karakesisoglou, I., Thevis, M., Weber, A.-A., Arnhold, S., and Addicks, K. (2008) Delta6-desaturase (FADS2) deficiency unveils the role of omega3- and omega6-polyunsaturated fatty acids. *EMBO J.* **27,** 2281–2292
35. Juneja, S. C., Barr, K. J., Enders, G. C., and Kidder, G. M. (1999) Defects in the germ line and gonads of mice lacking connexin43. *Biol. Reprod.* **60,** 1263–1270
36. Gerber, J., Weider, K., Hambruch, N., and Brehm, R. (2014) Loss of connexin43 (Cx43) in Sertoli cells leads to spatio-temporal alterations in occludin expression. *Histol. Histopathol.* **29,** 935–948
37. Carette, D., Weider, K., Gilleron, J., Giese, S., Dompierre, J., Bergmann, M., Brehm, R., Denizot, J.-P., Segretain, D., and Pointis, G. (2010) Major involvement of connexin 43 in seminiferous epithelial junction dynamics and male fertility. *Dev. Biol.* **346,** 54–67
38. Mazaud-Guittot, S., Meugnier, E., Pesenti, S., Wu, X., Vidal, H., Gow, A., and Le Magueresse-Battistoni, B. (2010) Claudin 11 deficiency in mice results in loss of the Sertoli cell epithelial phenotype in the testis. *Biol. Reprod.* **82,** 202–213
39. de Feijter, A. W., Matesic, D. F., Ruch, R. J., Guan, X., Chang, C. C., and Trosko, J. E. (1996) Localization and function of the connexin 43 gap-junction protein in normal and various oncogene-expressing rat liver epithelial cells. *Mol. Carcinog.* **16,** 203–212

40. Duffy, H. S., Delmar, M., and Spray, D. C. (2002) Formation of the gap junction nexus: binding partners for connexins. *J. Physiol. Paris* **96,** 243–249
41. Raschperger, E., Engstrom, U., Pettersson, R. F., and Fuxe, J. (2004) CLMP, a novel member of the CTX family and a new component of epithelial tight junctions. *J. Biol. Chem.* **279,** 796–804
42. Cohen, C. J., Shieh, J. T., Pickles, R. J., Okegawa, T., Hsieh, J.-T., and Bergelson, J. M. (2001) The coxsackievirus and adenovirus receptor is a transmembrane component of the tight junction. *Proc. Natl. Acad. Sci.* **98,** 15191–15196
43. Defamie, N., Berthaut, I., Mograbi, B., Chevallier, D., Dadoune, J.-P., Fénichel, P., Segretain, D., and Pointis, G. (2003) Impaired gap junction connexin43 in Sertoli cells of patients with secretory azoospermia: a marker of undifferentiated Sertoli cells. *Lab. Investig.* **83,** 449–456
44. Schwenk, F., Baron, U., and Rajewsky, K. (1995) A cre-transgenic mouse strain for the ubiquitous deletion of loxP-flanked gene segments including deletion in germ cells. *Nucleic Acids Res.* **23,** 5080–5081
45. Dymecki, S. M. (1996) Flp recombinase promotes site-specific DNA recombination in embryonic stem cells and transgenic mice. *Proc. Natl. Acad. Sci. U.S.A.* **93,** 6191–6196